Original Articles

Stress hormone-mediated acceleration of breast cancer metastasis is halted by inhibition of nitric oxide synthase

Renée L. Flaherty, Haya Intabli, Marta Falcinelli, Giselda Bucca, Andrew Hesketh, Bhavik A. Patel, Marcus C. Allen, Colin P. Smith, Melanie S. Flint*

School of Pharmacy and Biomolecular Sciences, University of Brighton, Centre for Stress and Age-related Disease, Moulsecoomb, Brighton, BN2 4GJ, UK

ABSTRACT

Stress hormones have been shown to be important mediators in driving malignant growth and reducing treatment efficacy in breast cancer. Glucocorticoids can induce DNA damage through an inducible nitric oxide synthase (iNOS) mediated pathway to increase levels of nitric oxide (NO). Using an immune competent mouse breast cancer model and 66CL4 breast cancer cells we identified a novel role of NOS inhibition to reduce stress-induced breast cancer metastasis. On a mechanistic level we show that the glucocorticoid cortisol induces expression of keys genes associated with angiogenesis, as well as pro-tumourigenic immunomodulation. Transcriptomics analysis confirmed that in the lungs of tumour-bearing mice, stress significantly enriched pathways associated with tumourigenesis, some of which could be regulated with NOS inhibition. These results demonstrate the detrimental involvement of NOS in stress hormone signalling, and the potential future benefits of NOS inhibition in highly stressed patients.

1. Introduction

Psychological stress induces an increase in the circulating levels of stress hormones, including the glucocorticoid cortisol [1]. Epidemiological evidence has associated negative psychosocial factors, including chronic stress, with increased incidence and poorer survival in breast cancer patients [2]. Furthermore, multiple studies have linked psychological stress with biological processes involved in metastasis [3–5], findings of particular importance since the primary cause of breast cancer-related death is metastatic spread [6].

Glucocorticoid signalling, mediated through the glucocorticoid receptor (GR), has been shown to promote tumourigenesis and drug-resistance in triple negative breast cancer (TNBC) [7], and increases in expression of GR in breast tumours have been correlated with decreased survival [8]. GR antagonism has also previously been shown to induce apoptosis and, in combination with conventional chemotherapies, reduce tumour size in models of TNBC [9]. We have previously explored the mechanistic actions of psychological stress in breast cancer, and shown that stress hormone exposure can induce DNA damage in breast cancer through the generation of reactive oxygen and nitrogen species (ROS/RNS). We have also previously shown that glucocorticoids mediate a non-genomic effect on inducible nitric oxide synthase (iNOS), the enzyme that generates NO, and increase nitric oxide (NO) signalling in

breast cancer cells [10]. Although iNOS is expressed in both ER + and ER-breast cancers [11,12], expression of iNOS has been found to correlate with tumour progression and poor survival in basal-like breast cancers [13,14], indicating that NO activity may drive malignant growth and spread. As such, iNOS represents a potential target to abrogate the detrimental effects of psychological stress hormone signalling.

Nitric oxide (NO) is an important signalling molecule modulating a range of functions within the cell, however the role of NO in tumour biology is complex and multifaceted [15]. Aspects of tumourigenic transformation can be driven by prolonged inflammation and exposure to high concentrations of NO, resulting in an increase in oxidative stress and subsequent DNA damage [16]. It is thought that NO may also be capable of driving transformation through the induction of angiogenesis and migration [17]. The highest concentrations of NO are produced by iNOS, and expression of iNOS has been shown to be positively correlated with tumour grade, stage and metastasis in breast cancer [11,18–20]. Several studies have shown that induction of iNOS expression in tumour cells promotes an increase in angiogenesis, and subsequently an increase in invasiveness and progression [16,21,22]. However transfection of iNOS in certain tumour types has been proven to inhibit growth, and when delivered as a gene therapy extends survival of metastases-bearing mice [23]. The biphasic effect of NO is

---

therefore dependent on localization, expression and activity of NOS isoforms as well as the concentration and length of exposure to NO.

Selective or non-selective inhibition of NOS as a potential therapy has been studied in relation to cancer, and has been shown to decrease angiogenesis, tumour growth and metastases and increase survival in breast cancers [14,16,22,24–26]. As such, our aim is to determine whether non-selective inhibition of NOS in the context of highly metastatic mammary tumours may abrogate the NO-mediated metastatic signalling induced by psychological stress.

2. Methods

2.1. Cells and culture conditions

The murine cell line 66CL4 (RRID:CVCL_9721), derived from a spontaneously-arising mammary tumour, were kindly donated by Dr Erica Sloan; Monash University Australia and maintained in MEM with 10% FBS (Gibco, UK). Human breast cancer cell line MCF-7 (RRID:CVCL_0031) was purchased from ATCC and maintained in Dulbecco's Modified Eagle Medium (DMEM) (Gibco, UK) with 10% FBS (Gibco, UK). MCF-7 cells were chosen as a comparator as they express similar levels of GR expression compared to human triple negative breast cancer (TNBC) cell lines [27] and also are known to express iNOS [12]. All cell lines were maintained in humid conditions at 37^OC and with 5% atmospheric CO_2. Cells were treated with hydrocortisone (Sigma Aldrich, UK) at a concentration of $5 \mu M$, and all other pharmacological agents as stated previously [10].

2.2. Electrochemistry

Electrodes were fabricated by modification of a previously published approach [28]. Characterisation was carried out as detailed previously [10]. 66CL4 and MCF-7 cells were plated at a density of 5×10^4 per well and incubated for 24 h. Cells were exposed to cortisol in the presence and absence of RU486, 1400 W dihydrochloride or L-NAME for 30mins prior to hormone treatment. Cells were immediately lysed and ROS/RNS levels were quantified using multiple-step amperometry using a stainless steel counter electrode and non-leak Ag|AgCl reference electrode. Measurements of the current were obtained at $+0.3$ V, $+0.45$ V, $+0.62$ V and $+0.85$ V for a duration of 30 s. The responses were analysed using approaches detailed in Ref. [29], using a CHI760E potentiostat (CH Instruments, Texas, USA).

2.3. Griess assay

66CL4 and MCF-7 cells were plated at a density of 3×10^5 per well of a 6 well plate. Cells were treated with cortisol in the presence or absence of RU486 or L-NAME for 30mins. Cell culture media was removed and assayed for extracellular nitrite using the Griess Reagent System (Promega, UK), as per the manufacturer's instructions.

2.4. Immunofluorescence

Cells were plated on glass coverslips and treated. Cells were then fixed in 3% paraformaldehyde 2% sucrose (pH 7.2) PBS for 10 min, washed, and permeabilized using 0.2% TritonX-100 in PBS for 2.5 mins at room temperature. Incubation with the primary antibody; anti-phospho-Histone H2AX (1:800 in 2% BSA) (Cell Signalling, RRID:AB_2118010), anti-RAD51 (1:200 in 2% BSA) (Cell Signalling, RRID:AB_2721109) or anti-GR (1:200 in 2% BSA) (Santa Cruz Biotech, RRID:AB_2155786) occurred for 45 min at 37^OC and the secondary antibody; anti-rabbit IgG FITC (1:200 in 2% BSA) (Sigma Aldrich, RRID:AB_259682) at 37^OC for 20 min. Fluorescent foci were detected using confocal microscopy (Leica, Germany) and positive cells, categorised as > 5 foci, expressed as a percentage of total cells counted.

2.5. In vivo study

All *in vivo* studies were carried out with Home Office approval and approved by the Animal Welfare and Ethical Review Body (AWERB) at the University of Brighton. All animal experiments comply with the ARRIVE guidelines and were carried out in accordance with the U.K. Animals (Scientific Procedures) Act, 1986. Female BALB/c mice were purchased at 6 weeks old from Envigo. They were housed 5 per cage with food and water *ad libitum* in a 12 h light/dark cycle. Mice were handled daily for 1 week prior to experimentation to acclimatise the mice to the investigator. Tumours were induced by the subcutaneous injection of 1×10^5 66CL4 cells were injected into the 4th mammary fat pad. Tumours were measured using digital callipers until they reached 150–200 mm^3, mice were then randomized into groups (n = 9). Groups were treated with intraperitoneal (IP) injections of saline or L-NAME (80 mg/kg dissolved in saline) (Sigma Aldrich, UK). To induce psychological stress a restraint stress model previously described [30] was used. Mice were individually placed in adequately ventilated 50 ml conical tubes for 2hrs 6 days a week for 2 weeks. Tumour volumes were measured twice a week using digital callipers and calculated using the formula for an ellipsoid sphere; volume (mm^3) = shortest (S) ^{2} x longest (L) x 0.52. Mice were also weighed once a week. Mice were sacrificed after 2 weeks of treatment. Animals that were sacrificed before the endpoint of the study due to tumour burden were excluded from the study. Primary tumours were weighed, dissected and cut in half, with half flash frozen in liquid nitrogen and half fixed in 10% neutral buffered formalin. Lungs were also removed, one half (lobe) was fixed in formalin and the other flash frozen in liquid nitrogen.

2.6. Bone marrow-derived macrophage isolation and culture

Female BALB/c 6–8weeks old were sacrificed and primary bone marrow-derived macrophages (BMDM) were isolated from the femurs and tibiae as described in Ref. [31]. BMDM's were cultured in RPMI-1640 with 10% FBS, 100 U/ml penicillin, 100 µg/ml streptomycin (Gibco, UK) and supplemented with 10 ng/ml M-CSF (Peprotech, UK). Growth media was changed on day 3, and on day 7 M-CSF was removed and BMDM were polarized to M1 by the addition of 100 ng/ml LPS (Sigma Aldrich, UK), or M2 by the addition of 10 ng/ml IL-4 (Peprotech, UK). Polarization was confirmed using qPCR to determine the expression of iNOS, arginase 1 (Arg1) and CCR2.

2.7. 3D spheroid Co-culture

66CL4 cells and polarized BMDM's were collected by scraping and 1×10^6 cells resuspended in 1 ml of serum free media. The lipophilic tracer dyes SP-DiOC$_{18}$(3) (66CL4) or DiL (BMDM) (Thermo Fisher, UK) were added at a concentration of 5 µg/ml and the cells incubated at 37^OC for 1hr. Cells were washed with PBS and combined in a ratio of 2000:1000 66CL4 to BMDM, or 2000 66CL4 cells alone in 30µl/well of a 96-well Ultra Low Attachment plate (Corning, UK). The plates were centrifuged at 300 g for 5mins and incubated at 37^OC and with 5% atmospheric CO_2 for 7 days. Each day media was removed and the spheroids treated with fresh media alone, cortisol 5 µM, L-NAME 100 µM or a combination or cortisol and L-NAME.

2.8. ELISA

The levels of CCL2 and IL-10 in the media from co-cultured 66CL4/BMDM spheroids was measured using a CCL2 or IL-10 ABTS ELISA kit (Peprotech, UK) as per the manufacturers instructions. Levels were normalised to protein extracted from the spheroids (mg/mL).

2.9. Immunohistochemistry

Formalin fixed tissues were processed using standard histological practices (Leica TP1050) and embedded into paraffin wax. For CD31 staining - Sections were dewaxed and subsequently transferred to antigen retrieval buffer (Tris/EDTA/Tween-20) at 95 °C for 20 min. Permeabilization (0.1% Triton-X in PBS) and blocking (2% BSA in PBS) followed. Sections were incubated with the primary antibody anti-CD31 (Abcam, RRID:AB_726362) and secondary anti-rabbit FITC conjugated (Sigma Aldrich, UK) for 1 h and 30 min at room temperature respectively. Areas of high microvessel density were identified at low magnification (×20), and at (x63) the number of small CD31-positive vessels were counted per field.

For KI67 staining - staining was performed Using Benchmark ULTRA autostainer (Ventana Medical Systems) as per the standard protocol. Slides were imaged at ×20 magnification using GXcapture software and KI67 labelling index analysed using ImmunoRatio [32]. Sections of fixed lungs were also taken through the midline and stained with Haematoxylin and eosin (H&E). Metastatic nodules were histologically identified at low magnification (×10) and counter per lung section.

2.10. qPCR

66CL4 cells were treated with cortisol for 30mins and 24hrs. RNA was extracted from cells and tissue using an RNeasy Kit (Qiagen, UK) and cDNA was synthesised using a Quantitect Reverse Transcription kit (Qiagen, UK) as per the manufacturer's instructions. A Rotor-Gene SYBR Green (Qiagen, UK) master mix was prepared according to the manufacturer's instructions using Quantitect Primer Assay for mouse *ACTB, NOS2, VEGFA, TWIST1, CCL2* and *ARG1* (Qiagen, UK). Ct values were obtained using Rotor-Gene Q software. Change in expression was measured using the ΔΔCt method and expressed as relative expression versus the experimental control or an internal universal reference.

2.11. Western blot

Cells were lysed in ice cold radioimmunoprecipitation assay (RIPA) buffer (150 mM NaCl, 1% 10 NP40/Igepal, 0.5% NaDoC, 0.1% SDS, 50 mM protease inhibitor (Sigma Aldrich, UK)) for 1–2 min. The lysates were subsequently spun at 13,000 g for 14 min at 4 °C. Protein concentration was determined using a DC protein assay (BioRad, UK) and 10 μg resolved on SDS-PAGE gels (10% resolving and 4.5% stacking) and transferred onto polyvinylidene fluoride (PVDF) membranes. Membranes were blocked in 5% BSA (Sigma Aldrich, UK) and incubated with the following primary antibodies; iNOS 1:2000 in 5% BSA (Santa Cruz, RRID:AB_2298577) and β-actin 1:10000 (Santa Cruz, RRID:AB_2714189) overnight at 4 °C, and appropriate secondary antibodies (Anti-rabbit/mouse IgG-HRP, Santa Cruz, RRID:AB_631746/RRID:AB_10915700) 1:2000 in 2.5% BSA for 1 h at room temperature. The membranes were developed using Amersham ECL Prime detection kit and exposed to Amersham Hyperfilm. The film was then processed using a developing system (Xograph Compact X4) and imaged in a Chemi Imager (Alpha Inotech).

2.12. Migration assay

66CL4 cells were transfected with *NOS2*-directed siRNA alongside a scrambled control (100 μM) (Qiagen, UK) using lipofectamine 2000 (10 μg/ml) (Fisher, UK) in Opti-MEM media (Gibco, UK). Cells were incubated overnight and replated at a density of 6×10^5 cells/well in MEM containing no FBS with or without cortisol (5 μM) onto transwell inserts (8 μM pores). The lower chamber was filled with MEM + 10% FBS and the cells incubated for 4 h. After 4 h inserts were removed, and cells that did not migrate on the top of the membrane were removed using a cotton swab. Cells on the underside were fixed with 3% PFA,

stained with Mayer's Haematoxylin and counted (x20). Data is expressed as cells per field.

2.13. Scratch assay

66CL4 cells were plated at a density of 1×10^5 in a 12 well plate and grown to confluencey. A 'scratch' was made using a p200 pipette tip and the cells treated with antagonists (RU486, L-NAME or 1400 W) for 30mins prior to the addition of cortisol. Images were taken at 0hrs and 24hrs. Area of the wound was measured using ImageJ and expressed as area closure relative to the 0hr time point.

2.14. Cell viability assay

66CL4 cells were plated at a density of 1×10^4 cells/well in a 96 well plate. Cells were treated with treated with antagonists (RU486, L-NAME or 1400 W) for 30mins prior to the addition of cortisol and incubated for 48hrs. Cell viability was determined by incubating the cells with 0.2 mg/ml MTT powder dissolved in cell culture media. Plates were protected from the light and incubated for 2 hrs at 37 °C. The MTT solution was removed and replaced with 200 μL dimethyl sulfoxide (DMSO), the plate shaken for 5mins and absorbance read at 495 nm (Digiread). Cell viability is expressed as a percentage of the control.

2.15. Transcriptomics

Total RNA was extracted from whole lungs flash frozen in liquid nitrogen immediately after removal from sacrificed animals. Lung tissues were immersed in RNA-later ice solution over night at 4 °C (Thermo Fisher Scientific, UK) to stabilize the mRNA populations prior to tissue homogenization. Lung tissues were homogenized in a Tissue Lyser (Qiagen, UK) 2×2 min at 30 rpm and centrifuged at 13.2 K rpm for 3 min to remove cell debris. Total RNA was extracted using RNeasy mini columns (Qiagen, UK) with an additional step of genomic DNA removal through agDNA eliminator column.

RNA was quantified using a Nanodrop One C spectrophotometer (Labtech International) and quality checked using an RNA Screen Tape on aTape Station instrument (Agilent Technologies). All the extracted RNAs used in the subsequent analysis had an RNA integrity number (RIN[e]) > 6. Total RNA (200 ng) was labelled with Cy3-CTP using the Low input Quick Amp One Color labelling kit (Agilent Technologies) and hybridized onto whole genome 8×60 K mouse microarrays v2 (AMADID 074809) following the manufacturer's instructions. The microarrays were washed and scanned using an Agilent microarray scanner G2505C.

Transcriptome data analysis - Raw scanned microarray images were processed using Agilent Feature Extraction software v11.5 and the data imported into R for normalization using the limma package [33]. Microarray data were background corrected using the 'normexp' method (with an offset of 50), quantile normalised and the data for technical replicates averaged. The processed data were then filtered to remove probes exhibiting low signals across the arrays, retaining non-control probes that are at least 10% brighter than negative control probe signals on at least three arrays. Data from identical replicate probes was then averaged to produce expression values at the unique probe level. Tests for differential expression were performed using the RankProd [34] package. Hierarchical clustering was performed by complete linkage clustering and using the Pearson correlation for the distance metric. Protein-protein interaction network construction and analysis, and functional enrichment analysis at the protein level, was undertaken in Cytoscape [35] (v3.6.1; using the STRING app (v1.4.0) [36] In STRING, confidence interaction scores of > 0.4 or > 0.7 were used to generate medium and high confidence networks, respectively.

2.16. Bioinformatic data mining

Kaplan-Meier survival curves for RFS and DMFS in breast cancer patients were generated using KMplotter [37], (http://kmplot.com/analysis/index.php?p=service). The Cancer Genome Atlas (TCGA) expression data according to breast cancer subtype was assessed and downloaded using TCGA Portal (tumorsurvival.org).

2.17. Other statistical analysis

Graphpad Prism v5.0 was used for the statistical analysis of all data other than the transcriptomics data described above. For qPCR a one sample *t*-test was performed on using 1 as the hypothetical value. For continuous data assuming normal variance a *t*-test or one-way analysis of variance was used with Tukey's multiple comparisons tests between groups. Statistical significance was determined where $p < 0.05$. All the results are representative of the mean of three or more independent experiments (n = 3) ± SEM unless otherwise stated.

2.18. Data availability

The transcriptomics datasets are deposited in the ArrayExpress database at EMBL-EBI (www.ebi.ac.uk/arrayexpress) under accession number E-MTAB-7299.

3. Results

3.1. Glucocorticoids increase ROS/RNS production and DNA damage in murine breast cancer cells

Increases in NO production, have the potential to activate oncogenic pathways and induce genetic instability through DNA damage [38]. The highly metastatic murine mammary carcinoma cell line 66CL4 was used as a model for aggressive triple negative breast cancer, and to validate previous findings in human breast cancer cell lines [10]. To characterise the acute glucocorticoid exposure ROS/RNS signature in 66CL4 cells; the cells were incubated with cortisol alongside the GR antagonist RU486, as well as the non-specific NOS inhibitor N-Nitroarginine methyl ester (L-NAME) and selective iNOS inhibitor 1400 W dihydrochloride (1400 W). Levels of intracellular nitrite, the stable by-product of nitric oxide was measured using electrochemical sensors, and extracellular nitrite by the Griess assay. Incubation with cortisol produced a significant increase in intracellular nitrite (Fig. 1A) which was reversed with the addition of iNOS blockers L-NAME, 1400 W and the GR antagonist, RU486. Similarly, extracellular levels of nitrite were increased in response to cortisol and a significant reduction was observed in response to RU486, 1400 W and L-NAME, and this was validated using the human breast cancer cell line MCF-7 (Fig. 1B). However, it should be noted that RU486 may also inhibit progesterone receptors present on MCF-7 cells [39]. To confirm the effects of glucocorticoids on nitrite production, the synthetic glucocorticoid dexamethasone (Dex) was also used to treat MCF-7 cells. Dex increased levels of nitrite in a similar manner, however no significant difference was observed between cortisol and dexamethasone treatment by either electrochemical detection or Griess assay (Supplementary Figs. 1A–B). 66CL4 cells were incubated with cortisol alongside GR antagonist RU486 and cells were immunofluorescently stained for the GR. In response to cortisol, translocation of the GR was observed and this was inhibited by RU486 (Supplementary Fig. 1C). The expression of the GR mRNA remains unchanged in response to glucocorticoids (Supplementary Fig. 1D). To further explore the potential contribution of stress hormone signalling to tumour invasiveness, 66CL4 cells were incubated with cortisol for 24hrs and the expression of iNOS, VEGF-A and Twist1 was examined using qPCR. A significant increase in mRNA levels of iNOS was seen after incubation in the presence of cortisol for 24hrs. A significant increase was also seen in expression of VEGF-A and

Twist1 after the addition of cortisol (Fig. 1C).

Previously glucocorticoids have been shown to induce DNA damage in human breast cancer cell lines. To assess cortisol-induced damage a marker of DNA damage, phosphorylated γ-H2AX foci, were visualised immunofluorescently in 66CL4 cells (Fig. 1D). In response to acute exposure to cortisol the percentage of foci positive cells was significantly increased, and this effect was inhibited by prior incubation with RU486 (Fig. 1E). RAD51 is involved in homologous recombination of double stranded DNA breaks. Elevated levels of RAD51 correlate with poor clinical outcome in certain breast cancers and RAD51 is often over expressed in human triple negative breast cancer cell lines [40]. RAD51 foci were examined in cells exposed to cortisol and a significant increase was observed, which was reversed with the addition of RU486 (Fig. 1F). These *in vitro* analyses demonstrate that murine mammary carcinoma cells respond to glucocorticoids in a similar manner to the human cell lines previously examined [10].

To determine if the effect of cortisol on cell migration was mediated through increased expression of iNOS, 66CL4 cells were transfected with siRNA directed towards *NOS2* (siNOS2) or a scrambled control (siControl) (Fig. 1G). Cortisol significantly increased the migration of siControl transfected 66CL4 cells through transwell membranes, and knockdown of iNOS negated the effect of cortisol on migration (Fig. 1H). Knockdown of *NOS2* also reduced the expression of the invasion-related genes *TWIST1* and *VEGFA* (Supplementary Fig. 1E). Furthermore, using the *in vitro* scratch assay as a measure of cell migration, treatment with cortisol was seen to promote migration, and this was reduced by inhibition of the GR and iNOS (Supplementary Fig. 1G). To determine if cortisol or inhibition of iNOS has effects on cell proliferation, 66cl4 cells were incubated with cortisol for 24 h alongside RU486, as well as L-NAME. None of the treatments had an effect on cell proliferation (Supplementary Fig. 1F). Taken together these results demonstrate that cortisol increases the invasive potential of mammary tumour cells, through increased expression of metastatic markers and NO signalling.
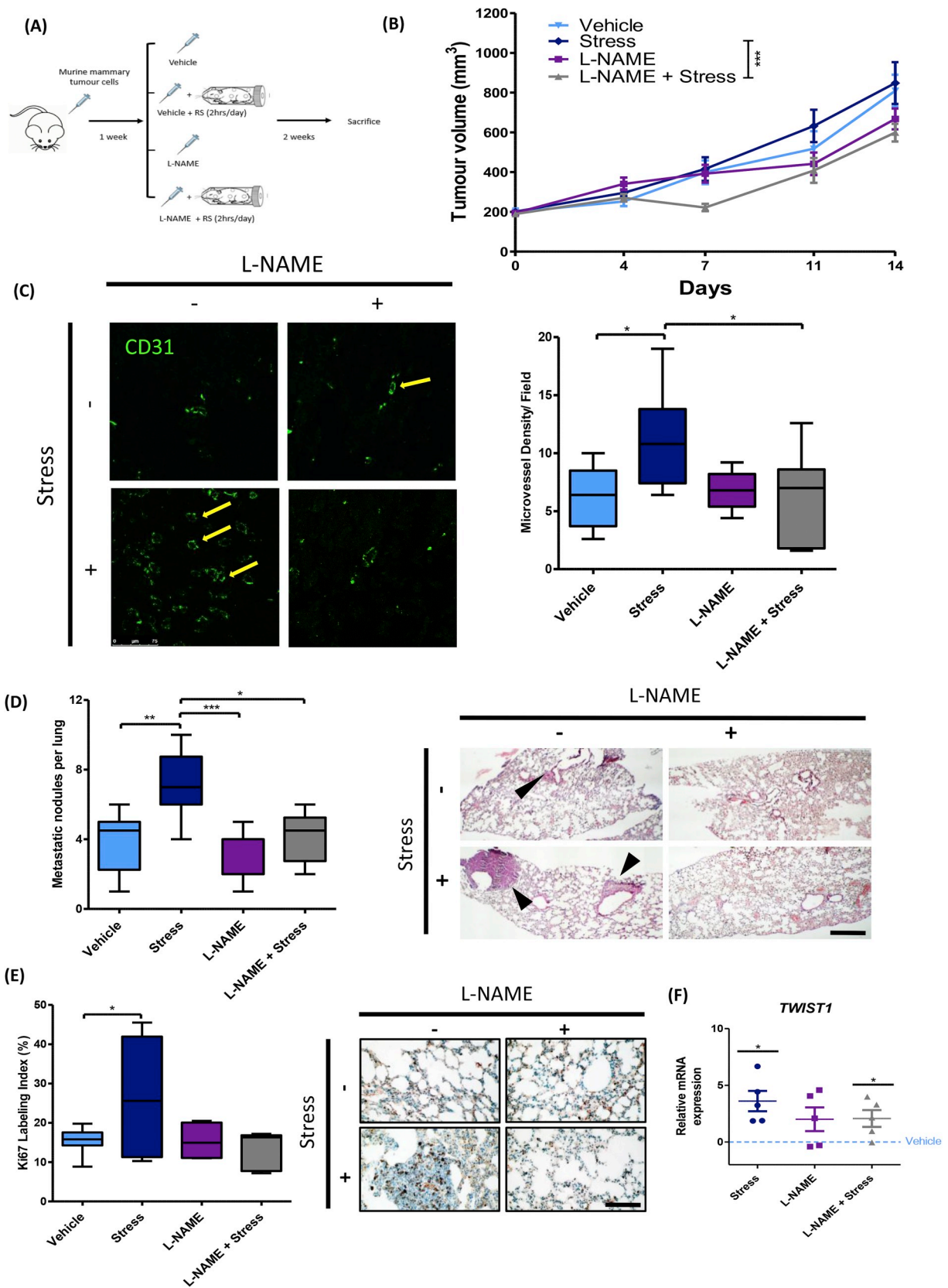
3.2. Inhibition of NOS reduces primary tumour growth and propensity for metastatic spread in stressed mice

A syngeneic mouse model of highly metastatic mammary tumours was used to examine the effects of psychological stress on tumourigenesis in combination with NOS inhibition. 66CL4 cells were chosen as their route of dissemination has been characterised as rapidly colonizing the lung but not liver, unlike 4T1 cells which colonise both [41]. Female mice bearing subcutaneous 66CL4 tumours were randomized into groups and underwent a program of restraint stress (RS) – a model of psychological stress known to induce sustained elevation of cortisol [42]. Groups were then further stratified into saline (vehicle) treated or L-NAME, the pan-NOS inhibitor treated mice (Fig. 2A).

There was no significant difference in tumour volume observed after 14 days between vehicle and L-NAME treated groups. In previous studies, reductions were seen after longer time courses as well as in combination with conventional chemotherapies [14]. There was also no difference in primary tumour volume between vehicle and stress groups, a normal observation in stress studies [43]. However, at 14 days a significant reduction in tumour volume was observed between the stress and L-NAME + stress groups (Fig. 2B). The weight of the primary tumours was also reduced in L-NAME treated groups, however not significantly so (Supplementary Fig. 2A). An increase in NO in the tumour microenvironment can stimulate microvascularisation [44,45], and it is therefore hypothesised that inhibition of NOS may serve as a regulator of angiogenic activity. To evaluate the degree of angiogenesis in the primary tumours, CD31 expression was immunofluorescently quantified as a measure of microvessel density. There was no difference in microvessel density between the vehicle and L-NAME treated groups. However, a significant increase in microvessel density was observed in the stress group compare to the vehicle treated, and this was
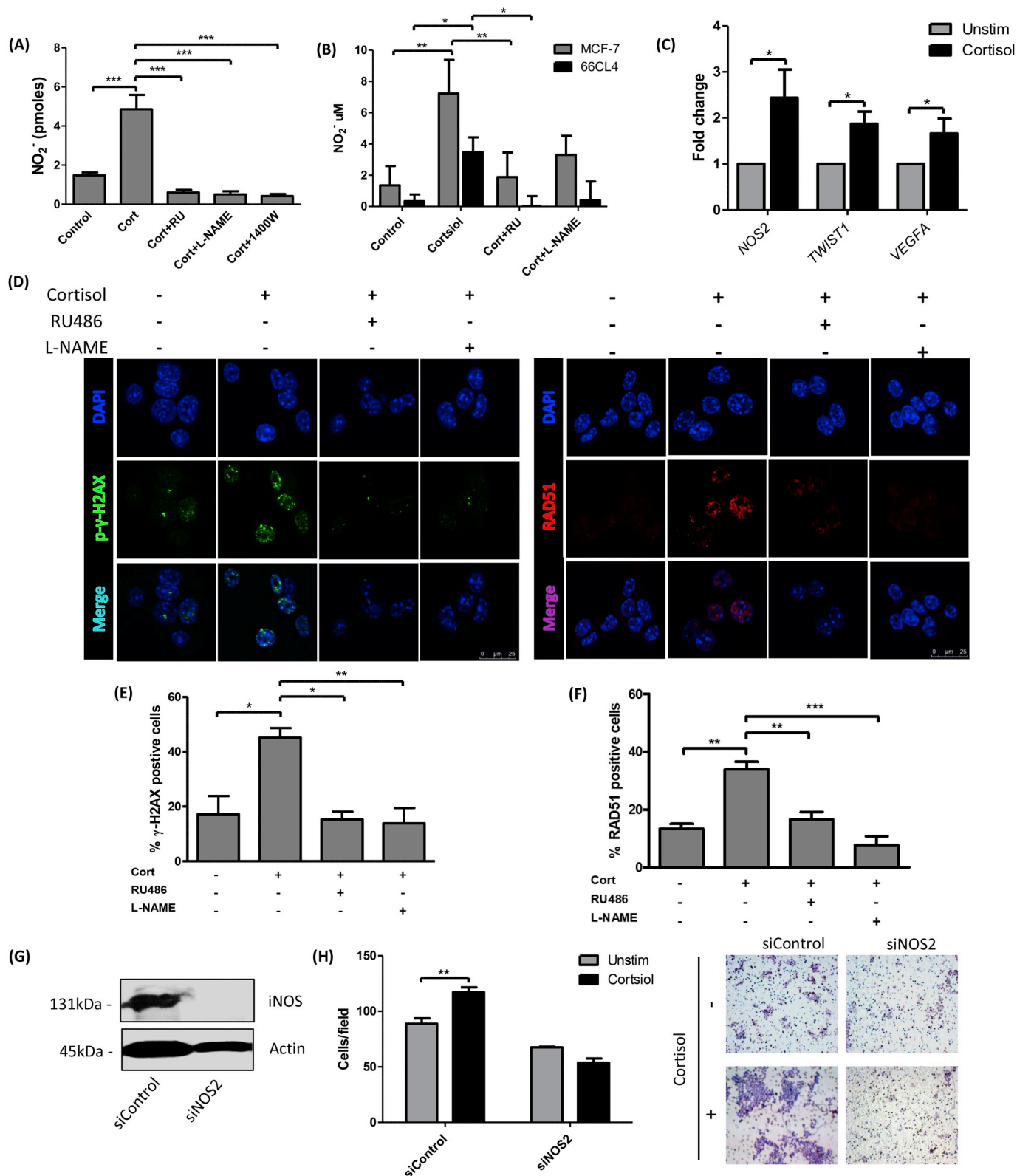
Fig. 1. Glucocorticoids increase ROS/RNS production and DNA damage in murine breast cancer cells. (A) 66CL4 cells were incubated with cortisol ± RU486, L-NAME and 1400 W. Levels of intracellular nitrite (NO_2) were measured using electrochemical sensors. **(B)** 66CL4 and MCF-7 cells were incubated with cortisol ± RU486 and L-NAME. Extracellular nitrite levels were quantified using the Griess assay. **(C)** 66CL4 cells were incubated with cortisol for 24hrs and the expression of *NOS2, VEGFA, TWIST1* and *ACTB* quantified using qPCR. Ct values were normalised against β-actin and fold change calculated using the delta-Ct method. **(D)** Cells were immunofluorescently stained for phosphorylated γ-H2AX and RAD51. Representative images shown. **(E–F)** Cells with > 5 foci were scored as positive and expressed as % of total cells. **(G)** 66CL4 cells were transfected with *NOS2*-directed siRNA (siNOS2) or scrambled control siRNA (siControl) and expression of iNOS quantified by Western blot. **(H)** siControl or siNOS2 transfected 66CL4 cells were plated onto transwell permeable supports and treated with cortisol for 4 h. Migrated cells were stained and counted. Data expressed as number of cells/field. Mean ± SEM expressed and statistical significance was determined one sample *t*-test, one way or two way ANOVA (post hoc Tukey's multiple comparisons). * = p < 0.05, ** = p < 0.01, *** = p < 0.001.

significantly reduced in the ʟ-NAME + stress group (Fig. 2C).

To examine the metastatic propensity of 66CL4 tumours in stressed mice, metastatic colonization of the lung was examined using

histopathology. Stressed mice had significantly more metastatic nodules per lung compared to vehicle treated mice, and in stressed mice treated with ʟ-NAME a significant reduction in metastatic lung

Fig. 2. Inhibition of NOS reduces primary tumour growth and propensity for metastatic spread in stressed mice. **(A)** 66CL4 mouse mammary tumour cells were transplanted into the fourth mammary fat pad of female BALB/C mice. Groups were exposed to restraint stress (2hrs/day) (n = 8) or no stress (Vehicle) (n = 9), in combination with L-NAME treatment (80 mg/kg) (n = 7). **(B)** Primary tumour volume. Data presented as mean ± SEM. **(C)** (Right) Primary tumours were immunofluorescently stained for CD31 expression, representative panels shown, (left) microvessel density was quantified and expressed as mean ± SEM. **(D)** Lungs were resected and sections taken midway through the lung were stained with H&E to quantify metastatic nodules. (Right) Arrows indicate metastatic nodules, representative panels shown, scale = 1 mm. **(E)** Lung sections were immunohistochemically stained for Ki67, and staining intensity quantified using ImmunoRatio. (Right) representative images shown. **(F)** RNA was extracted from a whole resected lung and the expression of *TWIST1* and *ACTB* quantified using qPCR. Ct values were normalised against β-actin and relative expression calculated using the delta-Ct method. Mean ± SEM expressed, for box-plots whiskers: min to max. Statistical significance was determined using one or two way ANOVA (post hoc Tukey's multiple comparisons). * = p < 0.05, ** = p < 0.01, *** = p < 0.001.

colonization was seen (Fig. 2D). The marker of proliferation Ki67 was quantified in the metastases, and a significant increase was also seen in stressed mice compared to vehicle treated (Fig. 2E). Twist1, a marker of metastasis which has been shown to promote metastatic seeding and spread in breast cancer [46,47], was quantified in the lungs of experimental mice. The expression of Twist1 was significantly elevated in the lungs of stressed mice compared to vehicle treated. Expression in stressed mice decreased with L-NAME treatment, although still remained significantly higher that vehicle treated (Fig. 2F).

3.3. Stress differentially regulates genes associated with tumourigenesis in the lungs of tumour-bearing mice

A transcriptomics analysis using microarrays was performed on the whole lungs of tumour-bearing mice to probe the effects of stress on metastatic spread by identifying stress-related changes in gene expression, and explore changes that can be reversed by L-NAME treatment (Fig. 3 and Supplementary data 2). The results identified 212 genes that are significantly upregulated in the stress group compared to the vehicle only control group, 18 of which are also significantly downregulated in the L-NAME + stress cohort compared to the stress only group (Fig. 3A). Functional analysis of the proteins encoded by the stress-induced transcripts indicates that stress provokes changes in gene expression associated with cell division, proliferation and chemotaxis (Fig. 3B and Supplementary data 2). Furthermore, of particular relevance were genes associated with cellular response to DNA damage, blood vessel development and cell migration. Indeed, a significant (p < 1.0e-16) protein-protein interaction (PPI) network derived from the *Mus musculus* medium confidence interactions curated in the STRING database [36] exhibits two connected sub-networks in the stress-induced gene products, that are centred on a highly connected group of proteins required for the mitotic cell cycle on the one hand, and cell chemotaxis and chemokine signalling on the other (Fig. 3B). As expected from the data in Fig. 2F the Twist1 transcription factor is in the group of genes identified as being significantly induced by stress, along with the related regulator Twist2. Hierarchical clustering of the microarray transcript abundance data for the stress-induced genes was used to identify groups of transcripts that are potentially co-regulated across the experimental conditions and revealed a group of 75 containing all 18 of the stress-induced transcripts identified as being responsive to correction by L-NAME (Fig. 3C). Analysis in STRING generated a significant PPI network (p = 1 × 10⁻¹³) with components integral to the control of the mitotic cell cycle and chemokine signalling, suggesting that L-NAME functions to ameliorate the effects of stress via perturbations in these processes (Fig. 3C). The aurora kinase protein A (AURKA) is prominent as one of the L-NAME reversible gene products identified in this analysis, and the network results suggest an important role in the mediation of the effects of stress on breast cancer. AURKA is required for correct progression through the mitotic cell cycle and has previously been implicated in tumourigenesis, with increased expression associated with migration and metastasis [48–50]. It is ca. 5-fold upregulated in the stressed mice, a change that is completely reversed by L-NAME (Supplementary Fig. 2B), and, since it is also among the top 3% of most highly connected proteins in the entire STRING mouse PPI network, this can be expected to generate extensive effects on cell function. CCR2 chemokine receptor binding proteins are significantly
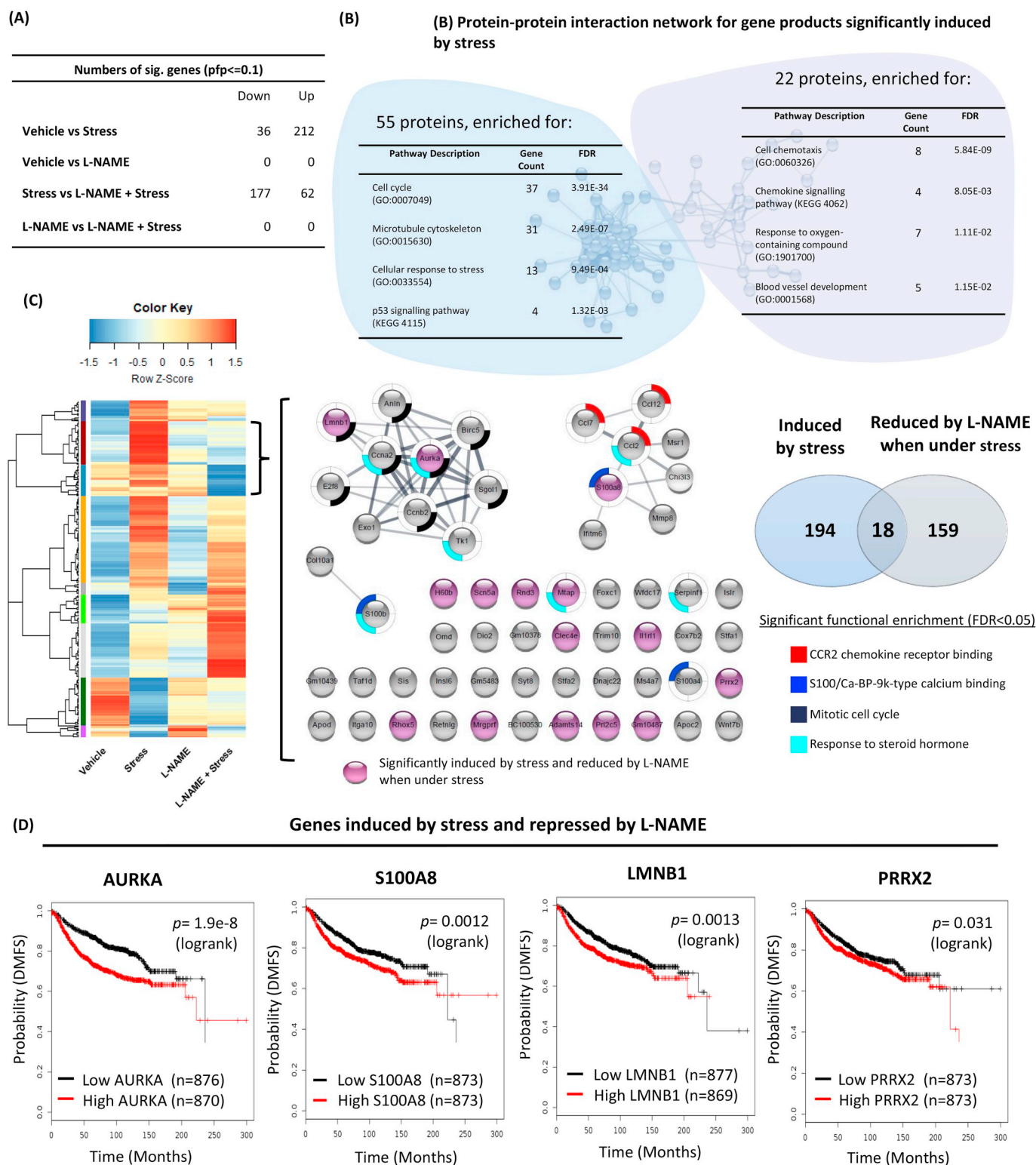
enriched in the network in Fig. 3C, including CCL2, CCL7, CCL12. Increases in expression of the CCL2 gene, encoding a monocyte chemoattractant, are associated with enhanced recruitment of infiltrating macrophages, promoting metastasis and correlating with poor overall survival [51]. In addition, Arg1, a marker of M2 macrophages [52] was significantly upregulated in the lungs from stressed mice. Furthermore S100/Ca-BP-9k-type calcium binding protein are also enriched. The S100A8 protein is secreted by monocytes during the inflammatory response and is highly expressed in aggressive breast cancers where it has been linked to the facilitation of invasion and metastasis [53,54]. S100A8, S100A4 and S100B are ligands for the Receptor for Advanced Glycation Endproducts (RAGE) and have been implicated in RAGE-dependent signalling that plays diverse roles in cell biology and disease processes, including inflammation, tumour outgrowth and metastatic colonization [53–55].

Of the 36 genes that are significantly downregulated in the stressed mice compared to the control group, only 2 are also significantly upregulated in the stress + L-NAME group compared to the stress only cohort (Supplementary data 1). The proteins encoded by the stress-repressed gene are significantly enriched for localization in the extracellular space (GO:0005615, p = 1.82E-08) and for functions associated with complement and coagulation cascades (KEGG 4610, p = 2.71E-05) and lipocalin binding (IPR002971, p = 7.56E-05).

Genes that were identified as being induced by stress - but repressed by L-NAME in the metastatic lungs of stressed mice - were also examined in relation to distant metastasis-free survival (DMFS) in breast cancer patients (Fig. 3D). Patients were not stratified into subtype as the GR can be expressed on both Luminal and HER2 + subtypes as well as basal. High expression of AURKA (p = 1.9e-8, logrank test) and S100A8 (p = 0.0012, logrank test) were significantly correlated with poor probability of DMFS. As was high expression of LMNB1 (p = 0.0013, logrank test), which encodes for lamin B1 and PRRX2 (p = 0.031, logrank test), a transcription factor related to EMT.

3.4. Stress associated genes are correlated with poor survival in invasive breast cancer subtypes

Glucocorticoids have been shown to regulate genes associated with breast cancer progression, including genes involved in neoplasm invasiveness and cell transformation [7]. The clinical importance of the glucocorticoid receptor (GR), as well as other genes linked to breast cancer progression such as Twist1 - a transcription factor identified as essential for the metastatic process [56] - was evaluated using survival analysis. The association between expression and recurrence-free survival (RFS) was investigated using gene expression and survival data from a publicly available microarray database (KM Plotter) [57]. Because we observed increases in NO₂⁻ in both TNBC and luminar A cell lines, cohorts were stratified according to intrinsic subtype (Basal-like, HER2, Luminal A, Luminal B) and further into high and low gene expression. Kaplan-Meier analysis shows high expression of GR correlates with lower probability of RFS in basal-like breast cancer (p = 0.021, logrank test; Fig. 4A), but not in HER2 (p = 0.17, logrank test; Fig. 1B), luminal A or B (Fig. 4C–D). Similarly, high expression of Twist1 was shown to correlate with significantly worse probability of RFS in basal-like (p = 0.0087, logrank test; Fig. 4A) and HER2 (p = 0.028, logrank test; Fig. 4B) breast cancers, but not luminal A or B (Fig. 4C–D).

(A)

Numbers of sig. genes (pfp<=0.1)		
	Down	Up
Vehicle vs Stress	36	212
Vehicle vs L-NAME	0	0
Stress vs L-NAME + Stress	177	62
L-NAME vs L-NAME + Stress	0	0

(B)   **(B) Protein-protein interaction network for gene products significantly induced by stress**

55 proteins, enriched for:

Pathway Description	Gene Count	FDR
Cell cycle (GO:0007049)	37	3.91E-34
Microtubule cytoskeleton (GO:0015630)	31	2.49E-07
Cellular response to stress (GO:0033554)	13	9.49E-04
p53 signalling pathway (KEGG 4115)	4	1.32E-03

22 proteins, enriched for:

Pathway Description	Gene Count	FDR
Cell chemotaxis (GO:0060326)	8	5.84E-09
Chemokine signalling pathway (KEGG 4062)	4	8.05E-03
Response to oxygen-containing compound (GO:1901700)	7	1.11E-02
Blood vessel development (GO:0001568)	5	1.15E-02

(C)

Induced by stress   **Reduced by L-NAME when under stress**

194   18   159

Significant functional enrichment (FDR<0.05)
- CCR2 chemokine receptor binding
- S100/Ca-BP-9k-type calcium binding
- Mitotic cell cycle
- Response to steroid hormone

Significantly induced by stress and reduced by L-NAME when under stress

(D)   **Genes induced by stress and repressed by L-NAME**

AURKA — *p*= 1.9e-8 (logrank) — Low AURKA (n=876), High AURKA (n=870)

S100A8 — *p*= 0.0012 (logrank) — Low S100A8 (n=873), High S100A8 (n=873)

LMNB1 — *p*= 0.0013 (logrank) — Low LMNB1 (n=877), High LMNB1 (n=869)

PRRX2 — *p*= 0.031 (logrank) — Low PRRX2 (n=873), High PRRX2 (n=873)

Fig. 3. Stress differentially regulates genes associated with tumourigenesis in the lungs of tumour-bearing mice. Transcriptomics analysis identifies changes in gene expression in the whole lungs of tumour-bearing mice subjected to combinations of confinement stress (Stress) and treatment with the NOS inhibitor L-NAME. (A) Numbers of significantly differentially expressed transcripts identified between the treatment groups using Rank Products analysis (Vehicle control group, n = 4; Stress, n = 3; L-NAME, n = 3; Stress + L-NAME, n = 3). Analysis of the overlap between the treatment groups identifies significant stress-related changes in transcription that are reversible by L-NAME treatment. Full details are provided in Supplementary data 1. **(B)** The 223 transcripts significantly upregulated in the lungs of stressed tumour bearing mice compared to the vehicle control group are enriched for functions associated with cell proliferation, chemotaxis and blood vessel development (see Supplementary data 1 for the complete analysis). A protein-protein interaction network derived from the *Mus musculus* medium confidence (0.4) interaction network in the STRING database shows two connected sub-networks in the stress-induced gene products. Only connected nodes are shown: the network for all nodes is significantly enriched for interactions compared to randomized sets, p-value $< 1 \times 10^{-16}$ **(C)**. Stress-induced transcripts that co-cluster with the 19 L-NAME responsive stress-induced transcripts generate a significant PPI network ($p = 1 \times 10^{-13}$) which suggests roles for Aurka, Ccl2 and certain S100 proteins (see also Supplementary data 1). **(D)** High/low expression of *AURKA, S100A8,* LMNB1 and *PRRX2* and distant metastasis-free survival (DMFS) was compared.
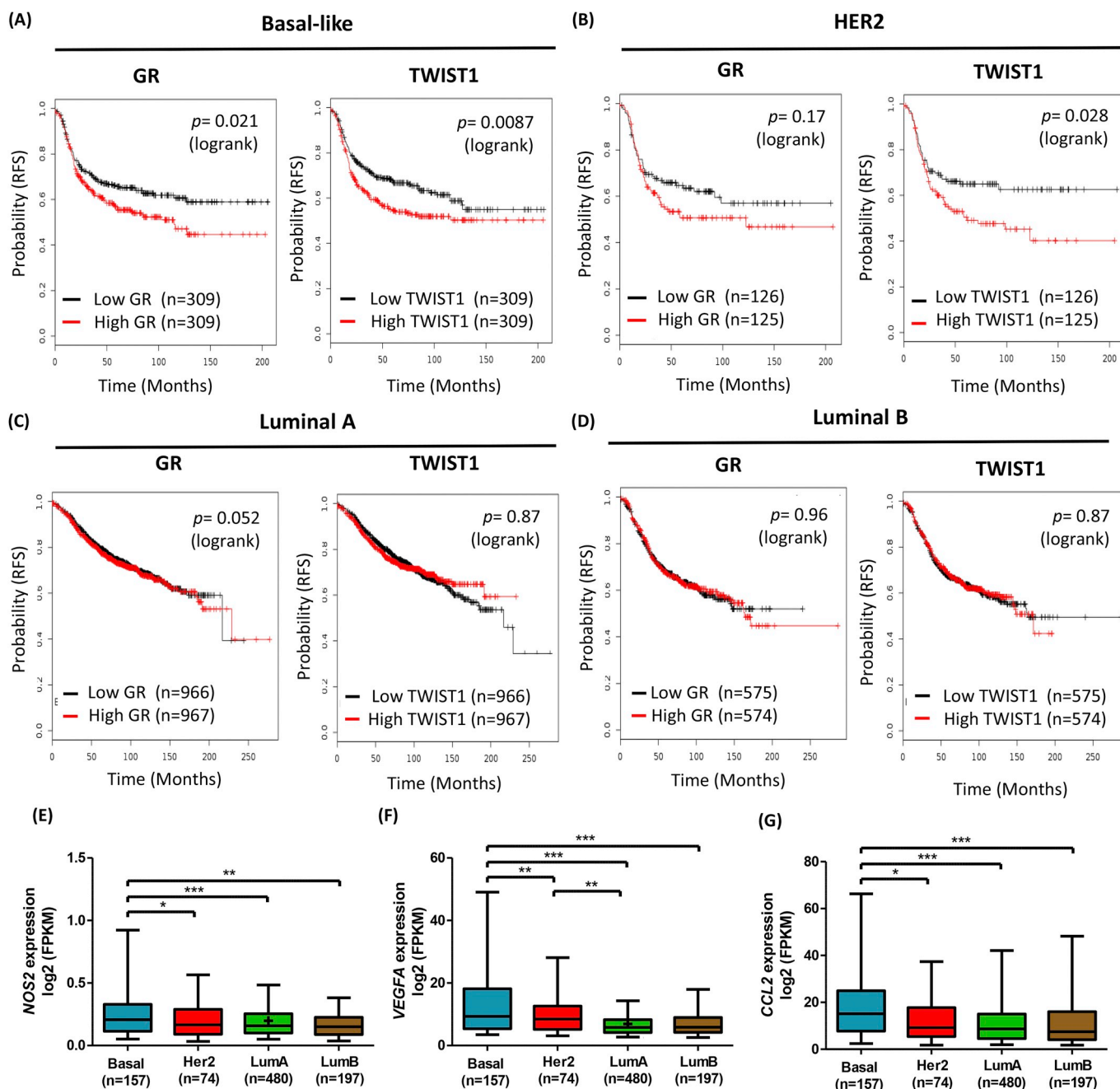
Fig. 4. Stress associated genes are correlated with poor survival in invasive breast cancer subtypes. Breast cancer microarray datasets were stratified into subtype; **(A)** Basal-like, **(B)** HER2, **(C)** Luminal A and **(D)** Luminal B, and further into high/low expression of NR3C1 (GR) or TWIST1, recurrence-free survival (RFS) was compared using Kaplan-Meier survival plots. Expression of **(E)** NOS2, **(F)** VEGFA and **(G)** CCL2 was examined in the TCGA data set of breast cancers (n = 908). Comparison of expression levels in intrinsic subtypes was carried out using one-way ANOVA and Tukey's multiple comparison test. Mean ± SEM expressed, for box-plots whiskers: 5–95 percentiles. Statistical significance was determined using one way ANOVA (post hoc Tukey's multiple comparisons). * = p < 0.05, ** = p < 0.01, *** = p < 0.001.

Increases in expression of iNOS in breast cancer have also been correlated with invasiveness and increased vascularization [21], and aberrant NO signalling is linked to induction of angiogenesis through stimulation of vascular endothelial growth factor (VEGF) [58,59]. Mining of the publicly available TCGA breast cancer dataset was carried out in relation to iNOS (*NOS2*) and *VEGFA,* genes closely involved in breast cancer progression. Expression of the chemokine CCL2 similarly implicated in breast cancer metastasis was also examined [60]. Comparison of the expression of *NOS2, VEGFA* and *CCL2* across intrinsic subtypes of breast cancer demonstrates that these genes are significantly associated with basal breast cancers compared to other

subtypes (Fig. 4E–G).

3.5. Cortisol promotes the release of pro-tumourigenic monocyte chemoattractants from breast cancer-macrophage co-cultures

Glucocorticoids have been shown to activate tumour associated macrophages (TAM's), which play a crucial role in tumour cell dissemination [61], as well as inducing polarization of macrophages to the pro-tumourigenic M2 phenotype [62,63], and upregulating anti-inflammatory mediators such as IL-10 which also promote TAM recruitment and activation [64,65]. In breast cancers the monocyte

66CL4

Bone marrow-derived macrophages
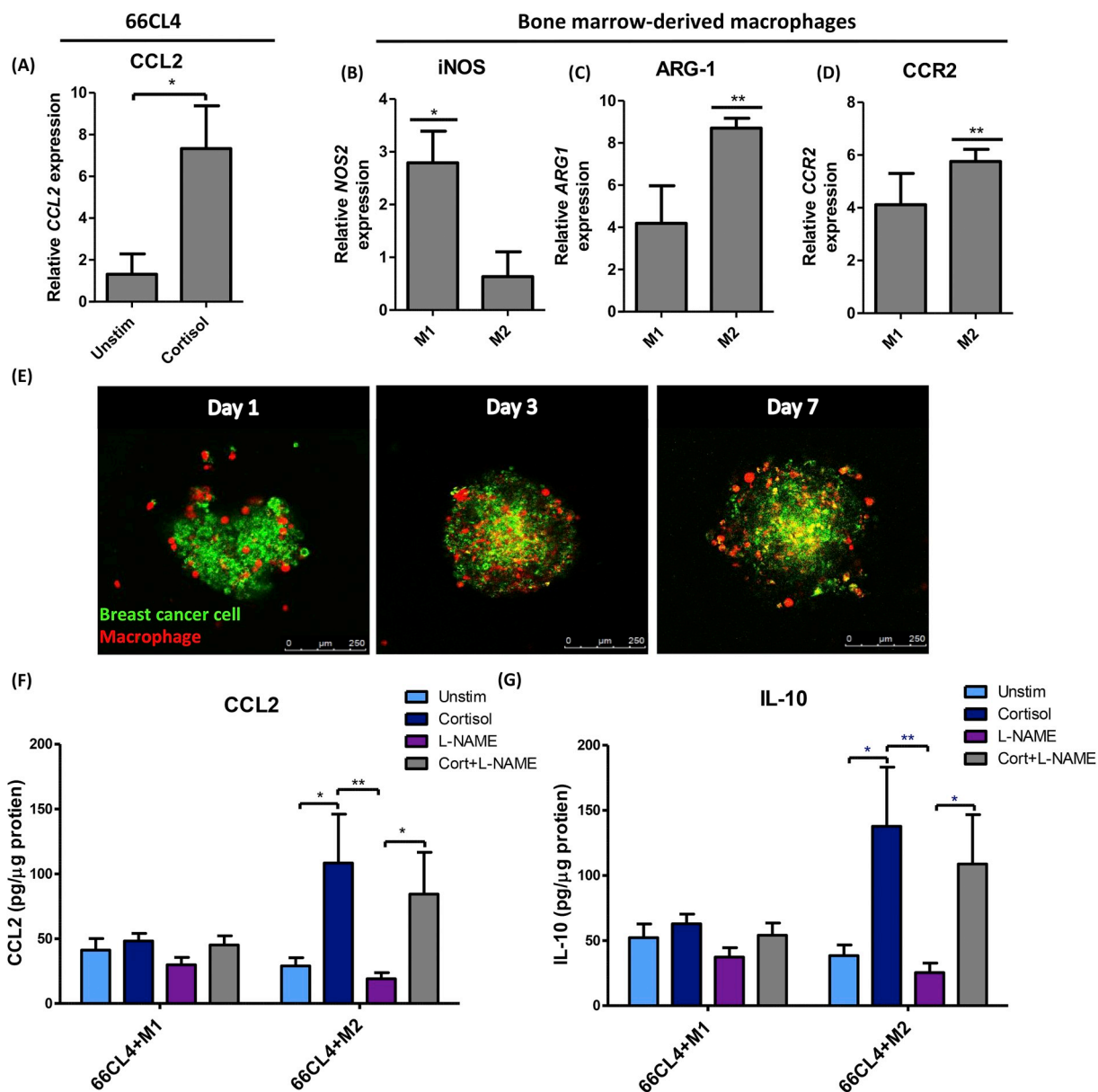
Fig. 5. Cortisol promotes the release of pro-tumourigenic monocyte chemoattractants from breast cancer-macrophage co-cultures. (A) 66CL4 cells were incubated with cortisol for 24hrs and the expression of *CCL2* and *ACTB* quantified using qPCR. **(B–D)** Bone marrow-derived macrophages (BMDM) were isolated, matured and polarized to M1 or M2. Markers of polarization (*NOS2, ARG-1*) and *CCR2* were quantified using qPCR. Ct values were normalised against β-actin and relative expression vs an internal reference calculated using the delta-Ct method. **(E)** Macrophages were co-cultured with 66CL4 breast cancer cells to form 3D spheroids, and incubated with cortisol ± L-NAME for 7 days. Representative images shown. **(F)** Media from the spheroid co-cultures was removed and assayed for CCL2 and IL-10 using ELISA. Levels were normalised to protein extracted from spheroids. Mean ± SEM expressed and statistical significance was determined using students t-test or two way ANOVA (post hoc Tukey's multiple comparisons). * = p < 0.05, ** = p < 0.01, *** = p < 0.001.

chemoattractant C–C Motif Chemokine Ligand 2 (CCL2), produced by tumour cells to recruit and polarize M2 macrophages, has been shown to correlate with decreased survival, as well an increase in angiogenesis and metastasis [46,51,66].

In murine breast cancer cells (66CL4) treatment with cortisol significantly increased the expression of CCL2 (Fig. 5A). In order to further investigate the role of glucocorticoids in potentially promoting metastasis through an immune-mediated mechanism, 3D heterospheroids were cultured using murine breast cancer cells and murine primary macrophages. Primary bone marrow-derived monocytes (BMDM) were isolated, matured and polarized to either M1 or M2 macrophages. Markers of polarization (M1 – iNOS, M2 – Arginase 1) were confirmed by qPCR (Fig. 5B–C). Expression of the receptor for CCL2, CCR2 was also significantly increased in M2 macrophages, but not M1, compared

to an internal control (Fig. 5D). Macrophages were combined with 66CL4 cells and grown as 3D heterospheroid co-cultures to model a tumour-TAM environment (Fig. 5E). Spheroids were treated with cortisol and L-NAME alone and in combination for 7 days and levels of CCL2 and IL-10 in the media were assayed. Cortisol treatment had no effect on levels of either CCL2 or IL-10 secreted by 66CL4 + M1 spheroids. However levels of both CCL2 and IL-10 were significantly increased in response to cortisol treatment of 66CL4 + M2 spheroids. As expected, inhibition of NOS using L-NAME had no effect alone, and in combination with cortisol did not affect the cortisol-induced release of CCL2 or IL-10 (Fig. 5F–G).
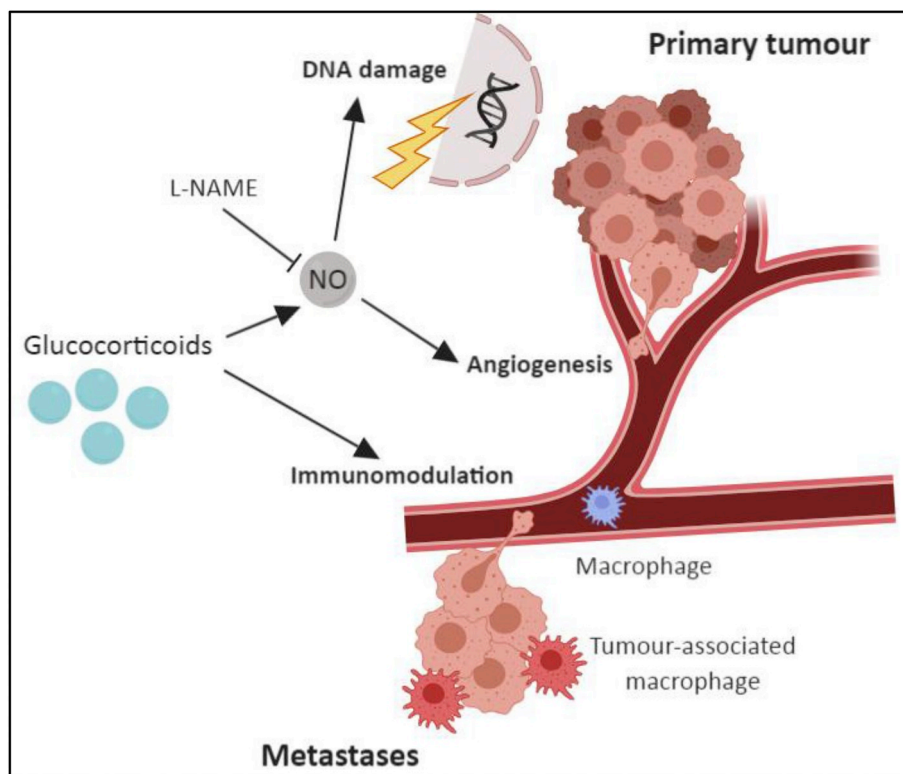
Fig. 6. Glucocorticoids promote metastatic dissemination through increased NO-mediated DNA damage and angiogenic signalling, as well as through immunomodulation.

4. Discussion

This study demonstrates the effects of glucocorticoids on pro-tumourigenic signalling and metastatic spread in breast cancer, and identifies a novel role for NOS inhibition.

The results show that the stress hormone cortisol increases the production of RNS and DNA damage through a NOS-mediated mechanism in mouse mammary tumour cells. A strong correlation has been shown to exist between oxidative stress, DNA damage and tumourigenesis, however there has been little conclusive evidence to suggest glucocorticoids exert a direct effect on this process. Previous work has shown acute exposure to cortisol stimulates the production of RNS in human breast cancer cell lines [10]. To confirm these effects would translate into an *in vivo* model of breast cancer, a mouse mammary tumour line was studied. Cortisol was able to activate the GR in mouse mammary tumour cells, and through GR activation increase levels of nitrite in a similar manner. Pharmacological inhibition of NOS was able to reverse cortisol-mediated nitrite production, and furthermore selective inhibition of iNOS proves that cortisol-induced generation of nitrite is facilitated through iNOS specifically. In the same cell line, DNA damage and repair, as evidenced by the formation of phosphorylated γ-H2AX foci and RAD51 foci, was also significantly increased in response to cortisol. Inhibition of NOS was able to negate the effect of cortisol on DNA damage indicating that the generation of NO is partly responsible for inducing DNA damage. Data from microarray analysis also reveals that in the lungs of stressed mice pathways pertaining to response to steroid hormone and response to DNA damage and were significantly enriched (Supplementary data 1). Taken together these results demonstrate the involvement of cortisol-regulated NO in DNA damage, and strengthens the hypothesis that one of the mechanisms through which exposure to glucocorticoids may influence tumourigenesis is through the upregulation of oxidative stress.

Furthermore, the *in vitro* data also demonstrates that not only does cortisol upregulate expression of iNOS, but also the expression of VEGF

and Twist1, two pro-metastatic markers heavily involved in the transformation to aggressive phenotypes. The deregulation of growth factor signalling is a hallmark of tumourigenesis, and is usually observed in invasive tumours [67]. The production and signalling of the potent angiogenic factor VEGF is often upregulated in the hypoxic tumour microenvironment and plays a role in the increased NO signalling within tumours. VEGF binding mobilizes intracellular calcium which induces eNOS and the production of NO, increasing the angiogenic potential by creating a feedback mechanism whereby VEGF induces NO, and NO in turn upregulates VEGF [58]. Therefore the increased NO signalling stimulated by glucocorticoids may serve to promote angiogenesis through VEGF in a chronic stress model.

In our study, we found that cortisol can increase NO production in luminal A MCF-7 cells, however although expression of GR correlated with lower probability of RFS in basal-like breast cancer it was not significant in other breast cancer subtypes as previously described [8].

In the syngeneic mouse model of breast cancer used in this study, daily restraint stress - a well characterised model of psychological stress - had no effect on primary tumour volume. This is in keeping with previous studies, and supports the view that stress hormone signalling does not directly affect primary tumour growth. The effects of chronic restraint stress on primary tumour volume are instead much more pronounced when combined with chemotherapy, with stress reducing the efficacy of chemotherapies in breast cancer [30], as well as in lung carcinoma [68]. Chronic stress alone has however been shown to affect the lymph vasculature surrounding the primary tumour, with restraint stress significantly increasing the lymphatic network and metastasis to the lymph node in a TNBC mouse model [5]. Similarly, in this study restraint stress significantly increased the microvasculature of the primary tumour compared to the control, indicating that whilst the tumours grew at the same rate, the primary tumours in stressed mice were more aggressive and had an increased propensity for metastasis. Inhibition of NOS was able to exert a significant effect on primary tumour growth when administered alongside restraint stress. There was a

significant reduction in primary tumour volume in the L-NAME + stress group compared to the stress alone, as well as a reduction in microvasculature indicating an inhibition of angiogenic NO signalling. As such the data gathered from this *in vivo* trial suggests that inhibition of NOS may be able to reduce the pro-tumourigenic effect of psychological stress in breast cancer, through reduction of NO-mediated angiogenesis. This is supported by the observation that stress significantly increased metastatic colonization of the lungs and cell proliferation, both of which were reduced by NOS inhibition.

However, whilst the inhibition of NOS alongside glucocorticoid treatment had effects on tumour cells and *in vivo*, NOS inhibition had no effect on the cortisol-induced release of pro-tumourigenic chemokines from breast cancer-macrophage spheroids. This may indicate a dual role for glucocorticoids in metastatic processes, by which glucocorticoids promote the pro-inflammatory and pro-tumourigenic release of NO from tumour cells, and the anti-inflammatory pro-metastatic recruitment of M2 macrophages, which is an NO independent process (Fig. 6).

Twist1, a transcription factor known to promote EMT, invasiveness and metastasis, was upregulated both *in vitro* in response to cortisol, and *in vivo* in the lungs of stressed mice. Furthermore, interrogation of breast cancer data sets identified expression of both the GR and Twist1 as markers of poor prognosis specifically in aggressive subtypes of breast cancer. This finding is consistent with a previous discovery that activation of the GR is associated with poor prognosis in ER-breast cancers, and is also linked to activation of epithelial-to-mesenchymal transition (EMT) pathways [8]. Increased NO signalling driven by an upregulation of iNOS expression in basal-like breast cancers can also activate oncogenic signalling networks that induce EMT [69]. The data presented therefore suggests a potential mechanism through which glucocorticoid signalling and can promote metastatic dissemination and modulation of the tumour microenvironment through increased NO signalling and upregulation of Twist1.

Interestingly, Twist1 has also been shown to modify the tumour microenvironment to promote angiogenesis and metastasis by inducing the secretion of CCL2, and subsequently attracting macrophages in a model of breast cancer [70]. Treatment with cortisol increased the expression of CCL2 in 66CL4 cells alone, and in 66CL4-macrophage spheroids this result was verified, with levels of CCL2 released significantly increasing as a result of cortisol treatment. It is unclear if in the experiments presented here, cortisol induces the production of CCL2 directly, or as a result of increased Twist1. However, the identification in the transcriptomics analysis of CCL2, as well as CCL7 and CCL12 as significantly induced in the lungs of stressed tumour-bearing mice provides further indication that stress can promote metastasis through macrophage signalling. This finding is in agreement with previous research detailing the role of β-adrenergic signalling on polarization of macrophages to an M2-like phenotype [71]. Indeed the both arms of the stress response have well characterised effects on immune function, with chronically elevated levels of glucocorticoids also having been shown to be immunosuppressive [3]. Glucocorticoids have also been shown to upregulate the expression of CCR2 - the receptor for CCL2, CCL7 and CCL12 - in human monocytes [72], and enhance the migratory potential of monocytes through upregulation of CCR2 [73]. The M2 marker Arginase 1 (Arg1) was also identified as significantly upregulated by stress in the lungs, suggesting that pro-tumourigenic M2 macrophages were being recruited as opposed to M1 macrophages [52,74].

Similarly our transcriptome analysis also identified S100A8, another signalling protein involved in macrophage-promoted tumour invasion, as being significantly induced by stress, an effect which was then negated by NOS inhibition using L-NAME. At metastatic sites macrophages can induce expression of S100A8, which enhances tumour cell migration and invasion, and acts as a marker of tumour aggressiveness [53]. Although not explicitly related to immune cell function, the same pattern of induction by stress and regulation by L-NAME was also observed with AURKA, which is also heavily implicated in metastatic

colonization in breast cancer [48,75]. Furthermore upregulation of paired-related homeobox1 (PRRX2), a transcription factor implicated in invasion and the induction of EMT, is seen in response to stress and reduced upon treatment with L-NAME. The stress-induced expression of these genes, and subsequent downregulation in stressed mice treated with L-NAME, coupled with evidence that high expression is correlated with poor probability of metastasis-free survival, indicates a mechanistic link between stress and metastasis in breast cancer. Furthermore, the data suggests stress is able to modulate the function of M2-like macrophages and alter cytokine signalling within the tumour microenvironment which promotes metastasis. This cytokine signalling is not blocked by L-NAME, however it may represent another potential new target for stress-mediated acceleration of cancer metastasis.

In conclusion, this study highlights new insights into the effect of stress hormone signalling on tumorigenesis in a model of invasive breast cancer, and the potential therapeutic benefit of NOS inhibition. This may be of relevance to highly stressed breast cancer patients, and especially to patients with aggressive cancer subtypes such as basal, where an increase in the expression of the GR and GR-mediated signalling may contribute to the spread of tumour cells.

Author contributions

MF participated in the design, conception, and coordination of studies and interpretation of the data and writing of the manuscript. RF prepared the manuscript, conducted the experiments and participated in the acquisition and interpretation of data. GB, AH and CPS participated in the design of the transcriptomics experiments. HI, MF, GB and AH assisted in the acquisition and interpretation of data and performed the statistical analysis. BAP designed, manufactured and characterised the sensors used. MCA and CPS contributed to data analysis. All authors read and approved the final manuscript.

Conflicts of interest

The authors have no conflict of interest to disclose.

Acknowledgements

Appendix A. Supplementary data

Supplementary data to this article can be found online at https://doi.org/10.1016/j.canlet.2019.05.027.

References

[1] T.M. O'Connor, D.J. O'Halloran, F. Shanahan, The stress response and the hypothalamic-pituitary-adrenal axis: from molecule to melancholia, Qjm-Monthly Journal of the Association of Physicians 93 (6) (2000) 323–333.
[2] Y. Chida, et al., Do stress-related psychosocial factors contribute to cancer incidence and survival? Nat. Clin. Pract. Oncol. 5 (8) (2008) 466–475.
[3] M. Moreno-Smith, S.K. Lutgendorf, A.K. Sood, Impact of stress on cancer metastasis, Future Oncol. 6 (12) (2010) 1863–1881.
[4] P.H. Thaker, et al., Chronic stress promotes tumor growth and angiogenesis in a mouse model of ovarian carcinoma, Nat. Med. 12 (8) (2006) 939–944.
[5] C.P. Le, et al., Chronic stress in mice remodels lymph vasculature to promote tumour cell dissemination, Nat. Commun. 7 (2016).
[6] A.J. Redig, S.S. McAllister, Breast cancer as a systemic disease: a view of metastasis, J. Intern. Med. 274 (2) (2013) 113–126.
[7] Z. Chen, et al., Ligand-dependent genomic function of glucocorticoid receptor in triple-negative breast cancer, Nat. Commun. 6 (2015) 8323.
[8] D. Pan, M. Kocherginsky, S.D. Conzen, Activation of the glucocorticoid receptor is associated with poor prognosis in estrogen receptor-negative breast cancer, Cancer Res. 71 (20) (2011) 6360–6370.
[9] M.N. Skor, et al., Glucocorticoid receptor antagonism as a novel therapy for triple-

negative breast cancer, Clin. Cancer Res.: an official journal of the American Association for Cancer Research 19 (22) (2013), https://doi.org/10.1158/1078-0432.CCR-12-3826.

[10] R.L. Flaherty, et al., Glucocorticoids induce production of reactive oxygen species/reactive nitrogen species and DNA damage through an iNOS mediated pathway in breast cancer, Breast Canc. Res. 19 (2017).

[11] S. Ranganathan, A. Krishnan, N.D. Sivasithambaram, Significance of twist and iNOS expression in human breast carcinoma, Mol. Cell. Biochem. 412 (1–2) (2016) 41–47.

[12] F. Bentrari, et al., Oct-2 forms a complex with Oct-1 on the iNOS promoter and represses transcription by interfering with recruitment of RNA PolII by Oct-1, Nucleic Acids Res. 43 (20) (2015) 9757–9765.

[13] S.A. Glynn, et al., Increased NOS2 predicts poor survival in estrogen receptor-negative breast cancer patients, J. Clin. Investig. 120 (11) (2010) 3843–3854.

[14] S. Granados-Principal, et al., Inhibition of iNOS as a novel effective targeted therapy against triple negative breast cancer, Breast Cancer Res. 17 (1) (2015) 527.

[15] T.A. Heinrich, et al., Biological nitric oxide signalling: chemistry and terminology, Br. J. Pharmacol. 169 (7) (2013) 1417–1429.

[16] D. Fukumura, S. Kashiwagi, R.K. Jain, The role of nitric oxide in tumour progression, Nat. Rev. Canc. 6 (7) (2006) 521–534.

[17] W.M. Xu, et al., The role of nitric oxide in cancer, Cell Res. 12 (5–6) (2002) 311–320.

[18] Y. Nakamura, et al., Nitric oxide in breast cancer: induction of vascular endothelial growth factor-C and correlation with metastasis and poor prognosis, Clin. Cancer Res. 12 (4) (2006) 1201–1207.

[19] B. De Paepe, et al., Increased angiotensin II type-2 receptor density in hyperplasia, DCIS and invasive carcinoma of the breast is paralleled with increased iNOS expression, Histochem. Cell Biol. 117 (1) (2002) 13–19.

[20] S. Loibl, et al., The role of early expression of inducible nitric oxide synthase in human breast cancer, Eur. J. Cancer 41 (2) (2005) 265–271.

[21] M. Vakkala, et al., Inducible nitric oxide synthase expression, apoptosis, and angiogenesis in in situ and invasive breast carcinomas, Clin. Cancer Res. 6 (6) (2000) 2408–2416.

[22] V. Kostourou, et al., The role of tumour-derived iNOS in tumour progression and angiogenesis, Br. J. Canc. 104 (1) (2011) 83–90.

[23] C.M. McCrudden, et al., Systemic RALA/iNOS nanoparticles: a potent gene therapy for metastatic breast cancer coupled as a biomarker of treatment, Mol. Ther. Nucleic Acids 6 (2017) 249–258.

[24] F. Vannini, K. Kashfi, N. Nath, The dual role of iNOS in cancer, Redox Biology 6 (2015) 334–343.

[25] B. Fitzpatrick, et al., iNOS as a therapeutic target for treatment of human tumors, Nitric Oxide 19 (2) (2008) 217–224.

[26] L.R. Kisley, et al., Genetic ablation of inducible nitric oxide synthase decreases mouse lung tumorigenesis, Cancer Res. 62 (23) (2002) 6850.

[27] M.S. Flint, et al., Induction of DNA damage, alteration of DNA repair and transcriptional activation by stress hormones, Psychoneuroendocrinology 32 (5) (2007) 470–479.

[28] Y. Li, et al., Electrochemical detection of nitric oxide and peroxynitrite anion in microchannels at highly sensitive platinum-black coated electrodes. Application to ROS and RNS mixtures prior to biological investigations, Electrochim. Acta 144 (2014) 111–118.

[29] A. Fagan-Murphy, et al., Electrochemical sensor for the detection of multiple reactive oxygen and nitrogen species from ageing central nervous system homogenates, Mech. Ageing Dev. 160 (2016) 28–31.

[30] A. Reeder, et al., Stress hormones reduce the efficacy of paclitaxel in triple negative breast cancer through induction of DNA damage, Br. J. Canc. 112 (9) (2015) 1461–1470.

[31] W. Ying, et al., Investigation of macrophage polarization using bone marrow derived macrophages, J. Vis. Exp.: J. Vis. Exp. (76) (2013) 50323.

[32] V.J. Tuominen, et al., ImmunoRatio: a publicly available web application for quantitative image analysis of estrogen receptor (ER), progesterone receptor (PR), and Ki-67, Breast Canc. Res. 12 (4) (2010) R56.

[33] M.E. Ritchie, et al., Limma powers differential expression analyses for RNA-sequencing and microarray studies, Nucleic Acids Res. 43 (7) (2015) e47.

[34] R. Breitling, et al., Rank products: a simple, yet powerful, new method to detect differentially regulated genes in replicated microarray experiments, FEBS Lett. 573 (1–3) (2004) 83–92.

[35] P. Shannon, et al., Cytoscape: a software environment for integrated models of biomolecular interaction networks, Genome Res. 13 (11) (2003) 2498–2504.

[36] D. Szklarczyk, et al., The STRING database in 2017: quality-controlled protein--protein association networks, made broadly accessible, Nucleic Acids Res. 45 (2017) D362–D368 Database issue.

[37] B. Gyorffy, et al., An online survival analysis tool to rapidly assess the effect of 22,277 genes on breast cancer prognosis using microarray data of 1,809 patients, Breast Canc. Res. Treat. 123 (3) (2010) 725–731.

[38] S. Ambs, S.A. Glynn, Candidate pathways linking inducible nitric oxide synthase to a basal-like transcription pattern and tumor progression in human breast cancer, Cell Cycle 10 (4) (2011) 619–624.

[39] A. Fazzari, et al., The control of progesterone receptor expression in MCF-7 breast cancer cells: effects of estradiol and sex hormone-binding globulin (SHBG), Mol. Cell. Endocrinol. 172 (1–2) (2001) 31–36.

[40] A.P. Wiegmans, et al., Rad51 supports triple negative breast cancer metastasis, Oncotarget 5 (10) (2014) 3261–3272.

[41] C.J. Aslakson, F.R. Miller, Selective events in the metastatic process defined by analysis of the sequential dissemination of subpopulations of a mouse mammary

tumor, Cancer Res. 52 (6) (1992) 1399.

[42] S. Gong, et al., Dynamics and correlation of serum cortisol and corticosterone under different physiological or stressful conditions in mice, PLoS One 10 (2) (2015) e0117503.

[43] R.A. Budiu, et al., Restraint and social isolation stressors differentially regulate adaptive immunity and tumor angiogenesis in a breast cancer mouse model, Cancer Clin. Oncol. 6 (1) (2017) 12–24.

[44] L.C. Jadeski, et al., Nitric oxide promotes murine mammary tumour growth and metastasis by stimulating tumour cell migration, invasiveness and angiogenesis, Int. J. Cancer 86 (1) (2000) 30–39.

[45] L.C. Jadeski, P.K. Lala, Nitric oxide synthase inhibition by N(G)-Nitro-l-Arginine methyl ester inhibits tumor-induced angiogenesis in mammary tumors, Am. J. Pathol. 155 (4) (1999) 1381–1390.

[46] B.Z. Qian, et al., CCL2 recruits inflammatory monocytes to facilitate breast-tumour metastasis, Nature 475 (7355) (2011) 222–225.

[47] J. Yang, et al., Twist, a master regulator of morphogenesis, plays an essential role in tumor metastasis, Cell 117 (7) (2004) 927–939.

[48] V. Eterno, et al., AurkA controls self-renewal of breast cancer-initiating cells promoting wnt3a stabilization through suppression of miR-128, Sci. Rep. 6 (2016) 28436.

[49] W. Siggelkow, et al., Expression of aurora kinase A is associated with metastasis-free survival in node-negative breast cancer patients, BMC Canc. 12 (2012) 562.

[50] A. Tang, et al., Aurora kinases: novel therapy targets in cancers, Oncotarget 8 (14) (2017) 23937–23954.

[51] L. Bonapace, et al., Cessation of CCL2 inhibition accelerates breast cancer metastasis by promoting angiogenesis, Nature 515 (2014) 130.

[52] S.M. Steggerda, et al., Inhibition of arginase by CB-1158 blocks myeloid cell-mediated immune suppression in the tumor microenvironment, Journal for immunotherapy of cancer 5 (1) (2017) 101-101.

[53] S.Y. Lim, et al., Tumor-infiltrating monocytes/macrophages promote tumor invasion and migration by upregulating S100A8 and S100A9 expression in cancer cells, Oncogene 35 (2016) 5735.

[54] C. Yin, et al., RAGE-binding S100A8/A9 promotes the migration and invasion of human breast cancer cells through actin polymerization and epithelial-mesenchymal transition, Breast Canc. Res. Treat. 142 (2) (2013) 297–309.

[55] A.R. Bresnick, D.J. Weber, D.B. Zimmer, S100 proteins in cancer, Nat. Rev. Canc. 15 (2) (2015) 96–109.

[56] Y. Xu, et al., Twist1 promotes breast cancer invasion and metastasis by silencing Foxa1 expression, Oncogene 36 (8) (2017) 1157–1166.

[57] A. Lanczky, et al., miRpower: a web-tool to validate survival-associated miRNAs utilizing expression data from 2178 breast cancer patients, Breast Canc. Res. Treat. 160 (3) (2016) 439–446.

[58] H. Kimura, H. Esumi, Reciprocal regulation between nitric oxide and vascular endothelial growth factor in angiogenesis, Acta Biochim. Pol. 50 (1) (2003) 49–59.

[59] T.E. Konopka, et al., Nitric oxide synthase II gene disruption - implications for tumor growth and vascular endothelial growth factor production, Cancer Res. 61 (7) (2001) 3182–3187.

[60] T. Kitamura, et al., CCL2-induced chemokine cascade promotes breast cancer metastasis by enhancing retention of metastasis-associated macrophages, J. Exp. Med. 212 (7) (2015) 1043.

[61] A. Schmieder, et al., Synergistic activation by p38MAPK and glucocorticoid signaling mediates induction of M2-like tumor-associated macrophages expressing the novel CD20 homolog MS4A8A, Int. J. Cancer 129 (1) (2011) 122–132.

[62] M.D. van de Garde, et al., Chronic exposure to glucocorticoids shapes gene expression and modulates innate and adaptive activation pathways in macrophages with distinct changes in leukocyte attraction, J. Immunol. 192 (3) (2014) 1196–1208.

[63] F.O. Martinez, S. Gordon, The M1 and M2 paradigm of macrophage activation: time for reassessment, F1000prime reports 6 (2014) 13-13.

[64] J. Ehrchen, et al., Glucocorticoids induce differentiation of a specifically activated, anti-inflammatory subtype of human monocytes, Blood 109 (3) (2007) 1265.

[65] C.B. Williams, E.S. Yeh, A.C. Soloff, Tumor-associated macrophages: unwitting accomplices in breast cancer malignancy, Npj Breast Cancer 2 (2016) 15025.

[66] E. Sierra-Filardi, et al., CCL2 shapes macrophage polarization by GM-CSF and M-CSF: identification of CCL2/CCR2-dependent gene expression profile, J. Immunol. 192 (8) (2014) 3858–3867.

[67] D. Hanahan, R.A. Weinberg, The hallmarks of cancer, Cell 100 (1) (2000) 57–70.

[68] S. Zorzet, et al., Restraint stress reduces the antitumor efficacy of cyclophosphamide in tumor-bearing mice, Brain Behav. Immun. 12 (1) (1998) 23–33.

[69] C.H. Switzer, et al., S-Nitrosylation of EGFR and Src activates an oncogenic signaling network in human basal-like breast cancer, Mol. Cancer Res.: MCR 10 (9) (2012) 1203–1215.

[70] J.M. Low-Marchelli, et al., Twist1 induces CCL2 and recruits macrophages to promote angiogenesis, Cancer Res. 73 (2) (2013) 662–671.

[71] D.M. Lamkin, et al., β-Adrenergic-stimulated macrophages: comprehensive localization in the M1-M2 spectrum, Brain Behav. Immun. 57 (2016) 338–346.

[72] M.P. Yeager, et al., Glucocorticoids enhance the in vivo migratory response of human monocytes, Brain Behav. Immun. 54 (2016) 86–94.

[73] M.P. Yeager, et al., Glucocorticoids enhance the in vivo migratory response of human monocytes, Brain Behav. Immun. 54 (2016) 86–94.

[74] P.J. Murray, et al., Macrophage activation and polarization: nomenclature and experimental guidelines, Immunity 41 (1) (2014) 14–20.

[75] A.B. D'Assoro, et al., The mitotic kinase Aurora–a promotes distant metastases by inducing epithelial-to-mesenchymal transition in ERalpha(+) breast cancer cells, Oncogene 33 (5) (2014) 599–610.